Material tests for the characterisation of replicated calcium silicate brick masonry

Jafari, Samira; Esposito, Rita

Publication date
2016

Document Version
Final published version

Citation (APA)
Jafari, S., & Esposito, R. (2016). *Material tests for the characterisation of replicated calcium silicate brick masonry*. Delft University of Technology.

Project number	C31B67
File reference	C31B67WP1-9
Date	November 14, 2016
Corresponding author	Samira Jafari (s.jafari@tudelft.nl)

TU Delft Large-Scale Testing Campaign 2016

MATERIAL TESTS FOR THE CHARACTERISATION OF REPLICATED CALCIUM SILICATE BRICK MASONRY

Authors: Samira Jafari, Rita Esposito

Lab collaborators: Andrea Maioli, Marina Damiola, Alessandro Pagani

***Cite as**: Jafari, S., Esposito, R. Material tests for the characterisation of replicated calcium silicate brick masonry. Report No. C31B67WP1-9, 14 November 2016. Delft University of Technology.*

This research work was funded by NAM Structural Upgrading stream

Table of Contents

1 Introduction

To characterise the mechanical properties of existing masonry, non/slightly destructive tests (NDT/SDT) can be performed in-situ or masonry samples can be collected to perform destructive tests (DT) in the laboratory. The in-situ tests aim to provide a quick-identification method for existing masonry, while laboratory tests are conducted to have a complete overview of the material behaviour (e.g. stress-strain relationships).

In order to provide reliable data, the pre-qualification of the companies to perform in-situ testing activities is of importance. Consequently a project, developed within the work package WP1a of the NAM Structural Upgrading project, has been set in cooperation with ARUP and EUCentre. The main aim of this work package is to qualify the companies. Additionally, the study of the correlation between DT and NDT/SDT results is investigated. NDT/SDT were performed by firms in the controlled laboratory environment on the calcium silicate brick masonry walls, built at TU Delft laboratory. Companion DT were performed by TU Delft. An overview of the material properties which can be achieved with the DT methods (in the scope of this project) is provided in Table 1. These obtained properties will be used to further investigate the correlation between NDT and SDT. Table 2 shows the correlation between the results obtained by NDT/SDT and DT methods.

All the tests were performed on replicated calcium silicate brick masonry. This masonry type was previously used in the large-scale testing campaign 2015, in which a complete material characterisation was made [1]. During the previous campaign two different construction phases took place:

- The first phase of construction took place in April and May 2015, with the aim of characterising the material properties as well as studying the behaviour of large-scale walls subject to quasi-static cyclic in-plane and out-of-plane tests.
- The second phase of construction took place in September 2015, with the aim of studying the behaviour of full-scale assemblage subject to quasi-static cyclic pushover test. As a result, companion samples for the compression and bond wrench tests were constructed.

In this report the results of the destructive material tests performed as companion material tests for the NDT/SDT are reported. These results are compared with the ones obtained in the large-scale testing campaign 2015 [1]. If comparison with previous test result is made, the results obtained in this project are named as third construction phase.

Table 1 – Destructive material tests for the characterisation of masonry.

<table>
<tr><th></th><th colspan="2">Type of test</th><th>Material property</th></tr>
<tr><td rowspan="4">Masonry</td><td>Compression</td><td>Vertical</td><td>Compressive strength
Young's modulus
Fracture energy in compression
Poisson ratio
Stress-strain relationship in compression (pre- and post-peak)</td></tr>
<tr><td rowspan="2">Shear test</td><td>Standard triplets</td><td rowspan="2">Initial and residual shear strength
Initial and residual shear friction coefficient
Mode-II fracture energy
Shear stress vs. shear displacement relationship (pre- and post-peak)</td></tr>
<tr><td>Modified triplets with head joints</td></tr>
<tr><td colspan="2">Bond wrench</td><td>Flexural bond strength</td></tr>
<tr><td>Masonry units</td><td>Compression</td><td>Single unit</td><td>Compressive strength of brick
Stress-strain relationship in compression</td></tr>
<tr><td rowspan="2">Mortar</td><td rowspan="2">Mortar bar</td><td>Compression</td><td>Compressive strength of masonry mortar</td></tr>
<tr><td>Bending</td><td>Flexural strength of masonry mortar</td></tr>
</table>

Table 2 – Correlation between the results of NDT/SDT and DT.

Type of test			Laboratory destructive test			
			Tests on brick	Tests on mortar	Compression test on masonry	Shear test on triplets
In-situ test	Non-destructive	Rebound hammer				
		Penetrometric				
		Ultrasonic				
	Slightly destructive	Single flat jack				
		Double flat jack				
		Shove test				

2 Nomenclature

2.1 Symbols

This report adopts mainly the nomenclature used in Eurocode 6 [2]. In addition, symbols used in the codes for testing are adopted.

α	Masonry (bed joint) angle of internal friction
α_{res}	Masonry (bed joint) residual angle of internal friction
ν	Poisson ratio of masonry
μ	Masonry (bed joint) coefficient of friction
μ_{res}	Masonry (bed joint) residual coefficient of friction
d_1	Distance between bearing supports
f_b	Normalised compressive strength of masonry unit
f_b^*	Compressive strength of masonry unit
f_m	Compressive strength of masonry mortar
f_{mt}	Flexural strength of masonry mortar
f_m'	Compressive strength of masonry in the direction perpendicular to the bed joints
f_p	Applied lateral pre-compression stress
f_{v0}	Masonry (bed joint) initial shear strength for standard triplet
f_{v0}^*	Masonry (bed joint) initial shear strength for modified triplet
$f_{v0,res}$	Masonry (bed joint) residual shear strength for standard triplet
$f_{v0,res}^*$	Masonry (bed joint) residual shear strength for modified triplet
f_w	Masonry uniaxial bond strength between the masonry unit and the mortar
l_j	Length of the mortar bed joint in a masonry specimens
l_m	Length of the mortar specimen
l_s	Length of the masonry specimen as built
l_p	Length of the loading plate for compression tests on mortar specimens
l_u	Length of the masonry unit as used in the construction of masonry
h_m	Height of the mortar specimen
h_s	Height of the masonry specimen as built
h_u	Height of the masonry unit as used in the construction
t_s	Thickness of the masonry specimen as built
t_m	Thickness of the mortar specimen
t_u	Thickness of the masonry unit as used in the construction of masonry
A_s	Cross sectional area of the specimen parallel to the bed joints (shear test)
E_{sb}	Elastic modulus of masonry unit calculated from compression tests on the stacked bricks
E_1	Secant elastic modulus of masonry subject to a compressive loading perpendicular to the bed

	joints, evaluated at 1/3 of the maximum stress
E_2	Secant elastic modulus of masonry subject to a compressive loading perpendicular to the bed joints, evaluated at 1/10 of the maximum stress
E_3	Chord elastic modulus of masonry subject to a compressive loading perpendicular to the bed joints, evaluated at between 1/10 and 1/3 of the maximum stress
E_{c1}	Cyclic stiffness evaluated in the cycle corresponding to a stress level equal to 0.07 of the expected maximum strength.
E_{c2}	Cyclic stiffness evaluated in the cycle corresponding to a stress level equal to 0.1 of the expected maximum strength.
E_{c3}	Cyclic stiffness evaluated in the cycle corresponding to a stress level equal to 0.25 of the expected maximum strength.
F_1	Applied vertical load (bond-wrench test)
F_2	Vertical load due to the weight of the top clamping system (bond-wrench test)
F_3	Vertical load due to the top masonry unit (bond-wrench test)
$F_{\max}$	Maximum vertical load
G_{f-c}	Fracture energy in compression for loading perpendicular to the bed joints
$G_{f\,II}$	Mode-II fracture energy in shear-compression test

2.2 Abbreviations

Avg.	Average
C.o.V.	Coefficient of variation
CS	Calcium silicate
LVDT	Linear variable differential transformer
St. dev.	Standard deviation
DT	Destructive test
NDT	Non-destructive test
SDT	Slightly destructive test

3 Construction of the samples

The masonry specimens were built in the Stevin II laboratory at the Delft University of Technology. The masonry was made of calcium silicate bricks and cement based mortar. The declarations of performance of the materials are reported in Appendix A.
Figure 1 shows the adopted masonry unit. Their dimensions are defined considering the orientation of the masonry unit as used in the construction of the masonry. This definition is consistently adopted in this report despite the position of the specimen in the test set-up. A similar consideration is applied to describe the dimensions of masonry specimens.

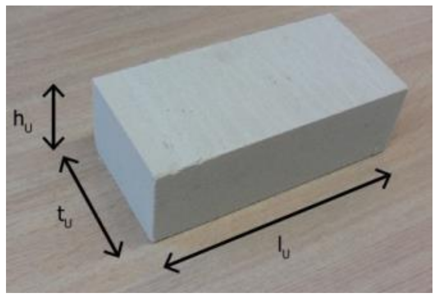

Figure 1 – Calcium silicate brick.

In order to ensure quality control, the construction followed the prescription as reported in the construction protocol [3]:

- The bags of mortar mix have been stored dry and separated from the soil;
- The mortar mix has been used within 18 months after production;
- The mortar has been mixed with clean water;
- The mortar has been prepared using a fixed water content;
- The flow of the mortar should be determined in agreement with EN 1015-3:1999 [4].
- At least three samples of mortar (size 160x40x40-mm^3) should be made at every start of the day during construction of masonry for testing the properties. The samples will be tested under flexural and compressive loading in agreement with EN 1015-11:1999 [5];
- The mortar has been prepared and used between 5 and 25 degrees;
- The mortar has been used within 2 hours after preparation;
- No additives have been mixed after preparation of the mortar;
- Bricks have been covered against moisture;
- Bricks were clean before use;
- Bricks have not been wetted before use;

The mortar was prepared with fixed water content per bag of mix (25 kg): 2.8 l/bag for calcium silicate masonry.

4 Compression strength of masonry unit

The compressive strength of a masonry unit (brick) is determined in agreement with EN 772-1:2000 [6].

4.1 Testing procedure

A single CS masonry unit having a length l_u, a height h_u and thickness t_u was used for the compression test in agreement with EN 772-1:2000 [6]. This test allowed determining the compressive strength of masonry unit (brick) (Figure 2). Six masonry unit specimens were subjected to the compression tests.

In order to estimate the Young's modulus of the masonry unit, four LVDTs were attached to the loading plates of the testing machine.

Figure 2 – Compressive test on the single masonry unit.

The test is carried out through a displacement-controlled apparatus including a hydraulic jack with 350-ton capacity. The hydraulic jack lifts a steel plate, the active side, and there is a passive load plate at the top. A hinge between the load cell and the top steel plate reduces possible eccentricities during loading. A load cell that measures the applied force is attached to the top steel plate. The masonry unit specimens were tested with its bed joint plane perpendicular to the loading direction.
The rate of the jack displacement was set to 0.01 mm/s to reach the maximum load in 2 min.

4.2 Experimental results

Assuming a linear stress distribution over the loaded cross section of the masonry unit, the compressive strength of the masonry unit f_b^* can be determined from test on single masonry unit as:

$$f_b^* = \frac{F_{\max}}{l_u . t_u} \tag{1}$$

where F_{max} is the maximum load, l_u and t_u are the length and thickness of the masonry unit respectively.
Following the Annex A of standard EN 772-1 [6], the normalised compressive strength of the masonry unit f_b is determined as:

$$f_b = \delta \cdot f_b^* \tag{2}$$

where δ is the shape factor determined in agreement with Table A.1 in Ref. [6].

Table 3 lists the compressive strength of the bricks as well as the normalised compressive strength obtained by tests on the single masonry unit. All the specimens failed in the compression tests by crushing.
In addition, the chord elastic modulus, evaluated between 1/10 and 1/3 of the maximum, are reported. The elastic modulus was calculated considering the LVDTs' reading. Comparing the average value of the elastic modulus with those results obtained in the last camping [1], through performing three-point bending tests on the single unit, it can be concluded that this method is not able to provide a proper estimation of the Young's modulus. As a result, tests on the stacked masonry unit adopted by Ad Vermeltfoort [7] will be conducted. The results of the tests will be included in the correlation report.

Table 3 – Compressive strength for the calcium silicate bricks.

Calcium silicate bricks				
Sample name	f'_b	δ	f_b	E_b
	MPa	-	MPa	MPa
TUD_MAT-B11a	20.5	0.707	14.5	4184
TUD_MAT-B11b	17.9	0.707	12.6	3881
TUD_MAT-B11c	15.1	0.707	10.7	2377
TUD_MAT-B11d	17.2	0.707	12.2	4239
TUD_MAT-B11e	20.8	0.707	14.7	2767
TUD_MAT-B11f	21.1	0.707	14.9	5247
Average	**18.76**	**-**	**13.26**	**3783**
Standard deviation	**2.42**	**-**	**1.71**	**1052**
Coefficient of variation	**0.13**	**-**	**0.13**	**0.28**

5 Flexural and compressive strength of mortar

During the masonry construction, mortar samples were collected and cast in moulds to be tested for the flexural and compressive strength in agreement with EN 1015-11:1999 [5].The consistency of the mortar was determined in accordance with EN 1015-3:1999 [4].

5.1 Testing procedure

During each day of construction, at least three mortar specimens having a length of l_m = 160 mm, a height of h_m = 40 mm and thickness of t_m = 40 mm were collected. The samples were stored in controlled conditions. The first two days they were placed in a fog room (T = 20 ± 2 °C, RH = 95 ± 5%) with the moulds. After two days, they were unmoulded and kept for other five days in the fog room. Eventually, they were placed in a conditioning room with a temperature of 20 ± 2 °C and a relative humidity of 50 ± 5 % until testing. The test was performed after at least 28 days from construction.

The flexural strength was determined by three-point bending test (Figure 3a). The test set-up is composed by two steel bearing rollers having a diameter of 10 ± 0.5 mm and spaced d_1 = 100 ± 0.5 mm. A third roller is centrally placed on top of the sample to apply the load.

The compression test was performed on the broken pieces obtained from the flexural test, which have at least a length of 40 mm. The specimen is placed between two steel plates with a length of l_p = 40 mm. For the interpretation of the results the specimens considered to be 40x40x40-mm (Figure 3b).

For both test, the load was applied without shock at a uniform rate so that failure occurred within a period of 30 to 90 s. The maximum load was recorded.

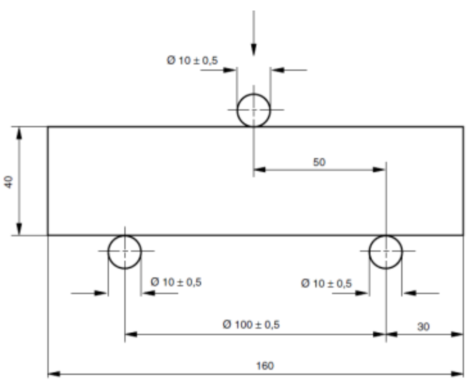

(a)

(b)

Figure 3 – Test on masonry mortar specimens: (a) three-point bending test; (b) compression test.

5.2 Experimental results

The flexural strength f_{mt} of the mortar was calculated as [5]:

$$f_{mt} = \frac{3}{2}\frac{F_{\max} d_1}{t_m h_m^2} \qquad (3)$$

where F_{max} is the maximum load, d_1 is the distance between the supports (100 mm ± 0.5 mm), h_m is the height of the mortar specimen (40 mm) and t_m is the thickness of the mortar specimen (40mm).
The compressive strength f_m of the mortar was calculated as [5]:

$$f_m = \frac{F_{\max}}{t_m l_p} \qquad (4)$$

where F_{max} is the maximum load, t_m is the thickness of the mortar specimen (40 mm) and l_p is the length of the loading plate (40 mm).

During the masonry construction, the slump flow tests were performed when a new batch of mortar was prepared. The diameter of the cone was obtained by the flow test described in EN 1015-3:1999 [4]. The measured diameter varied between 147 to 163 mm (see Table 4). As to follow the previous construction procedure, the same amount of water (2.8 l/bag) was used; although the flow results were lower than those measured in the previous construction phases (see Table 6).

Aside from the large walls and the companion samples constructed with the aim of testing for the scope of WP1a, one large-scale CS brick wall (COMP20) also was prepared to be tested for the research purpose of WP3. It should be mentioned that the NDT5 wall was tested by SGM and the NDT4 wall was tested by NEBEST.

Table 4 – Consistency of calcium silicate masonry mortar measured during the third phase of construction in Aug. 2016.

Date	Cast	Flow (mm)
16-8-2016	1	153
	2	163
	4	163
17-8-2016	1	162
	2	157
	3	151
18-8-2016	1	156
	2	157
	3	158
	4	154
	5	155
	6	152
19-8-2016	1	149
	2	153
	3	149
	4	159
22-8-2016	1	147
	2	154
	3	155
	4	157
23-8-2016	1	147
	2	154
	3	157
	4	163
Average		**155**

The flexural and compression tests on the hardened mortar were performed at least after 28 days. Table 5 lists the results for the three-point bending tests and compression tests. Three-point bending tests were performed on 75 specimens and compressive tests were conducted on 150 specimens. The mortar has a compressive strength of 7.6 MPa and flexural strength of 3.2 MPa. In both cases, the coefficient of variation is limited to less than 10%.

Table 6 compares the results of tests on the fresh and hardened mortar constructed at the three phases of constructions at TU Delft. There is a slightly differences between the flexural strength values of the mortar produced during the three phases of construction. It should be mentioned that although the mortar used for the construction of the samples were taken from the same batch, the aging of the cement (around 13 to 15 month), environmental conditions and the mixing procedure can influence the mortar properties. Figure 4 shows the statistical distribution of flexural and compressive strength of mortar in three different construction phases.

Table 5 – Flexural and compressive strength of calcium silicate masonry mortar constructed in Aug. 2016.

Date	Companion samples	Cast	Flexural tests			Compression test		
			f_{mt} (MPa)	St. Dev.	C.o.V.	f_m (MPa)	St. Dev.	C.o.V.
16-8-2016	MAT-16A	1	3.3	0.19	0.06	7.9	0.46	0.06
	MAT-16B	2	2.5	0.18	0.07	5.3	0.27	0.05
	MAT-11	4	3.1	0.11	0.03	7.3	0.36	0.05
17-8-2016	MAT-11	1	3.0	0.11	0.04	6.6	0.41	0.06
	NDT5	2	3.5	0.10	0.03	7.1	1.92	0.27
	NDT5	3	3.0	0.10	0.03	6.8	0.42	0.06
18-8-2016	NDT5	1	3.1	0.13	0.04	7.9	0.29	0.04
	NDT5	2	3.4	0.06	0.02	7.8	0.64	0.08
	NDT5	3	3.1	0.05	0.02	7.0	0.95	0.14
	NDT4	4	3.0	0.32	0.11	7.7	0.28	0.04
	NDT4	5	3.2	0.29	0.09	8.7	0.44	0.05
	NDT4	6	3.1	0.17	0.06	7.0	0.14	0.02
19-8-2016	NDT4/COMP20	1	3.3	0.38	0.12	7.4	0.29	0.04
	NDT4	2	3.5	0.17	0.05	8.1	0.28	0.03
	NDT3/ COMP20	3	3.2	0.10	0.03	8.6	0.34	0.04
	NDT3/ COMP20	4	3.7	0.36	0.10	9.0	0.37	0.04
22-8-2016	NDT2	1	2.7	0.02	0.01	5.7	0.29	0.05
	NDT2	2	2.7	0.18	0.07	7.1	0.26	0.04
	NDT2	3	3.4	0.21	0.06	8.2	0.70	0.09
	NDT2	4	3.4	0.15	0.04	8.5	0.32	0.04
23-8-2016	NDT2/1	1	3.3	0.10	0.03	7.4	0.24	0.03
	NDT1	2	3.6	0.18	0.05	8.8	0.30	0.03
	NDT1	3	3.4	0.27	0.08	7.5	0.56	0.07
	NDT1	4	3.4	0.30	0.09	8.4	0.43	0.05
Average all casts			**3.21**			**7.57**		
Standard deviation			**0.18**			**0.46**		
Coefficient of variation			**0.05**			**0.06**		

Table 6 – Comparison between the results of tests on fresh and hardened mortar at three phases of construction.

Period of construction	Flow	Flexural strength	Compressive strength
	(mm)	MPa	MPa
First phase (Apr/May 2015)	174	2.79 [0.08]	6.59 [0.10]
Second phase (Sept. 2015)	162	3.56 [0.05]	7.24 [0.08]
Third phase (Aug. 2016)	155	3.21 [0.05]	7.57 [0.06]

The coefficient of variation is presented between brackets.

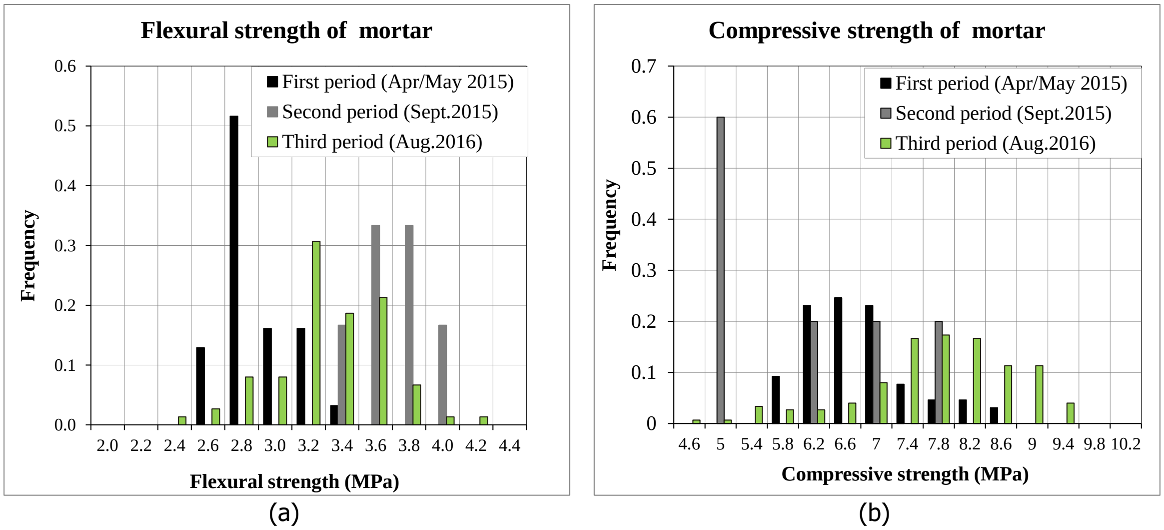

Figure 4 – Statistical distribution of mortar strength: (a) flexural strength; (b) compressive strength.

6 Compression strength of masonry

The compression strength and elastic modulus of the masonry were determined in agreement with EN 1052-1:1998 [9]. Additional test configuration was adopted to investigate the cyclic response of the material, to have the same testing procedure adopted in double flat jack tests [10].

6.1 Testing procedure

The size of the specimens was determined on the basis of the masonry units [9]. The calcium silicate masonry specimens have dimensions of 434x476x102-mm (2x6x1-brick). A 10 mm thick layer of gypsum was applied to faces in contact with the loading plates, to ensure that the loaded faces of the specimens are levelled and parallel to one another. This is done to prevent additional stresses in the specimens.

The compression strength and elastic modulus of the masonry were determined in a vertical configuration in which the loading was perpendicular to the bed joints. The test is prescribed by the standard EN 1052-1:1998 [9].

The testing apparatus was provided with a 3500 kN hydraulic jack, positioned at the bottom. The hydraulic jack lifts a steel plate, the active side, and there is a passive load plate at the top. A hinge between the load cell and the top steel plate reduces possible eccentricities during loading. The hydraulic jack is operated in deformation control, using the displacement of the jack as control variable. A load cell that measures the applied force is attached to the top steel plate (Figure 5a).

Four LVDTs (two for each side) are attached to the specimen to register vertical relative displacements over the height of the specimen (Figure 5b). They are installed as closely as possible to the surface of the specimen to reduce possible errors caused by rotation of the contact points to which they are attached. Their measuring range is 10 mm with an accuracy of 0.5%. Additionally, two LVDTs (one for each side) are attached to the specimen to register the horizontal relative displacement over the length of the specimen. Their measuring range is 10 mm with an accuracy of 0.5%.

Three specimens were tested by applying a *monotonic loading* as prescribed by the EN 1052-1:1998 [9] (Figure 6). Half of the expected maximum compression force is applied in three equal steps and was kept constant for 2 ± 1 min. Afterwards, the maximum stress in reached monotonically. Subsequently, the test was continued to explore the post-peak behaviour. The load was applied with a rate of 0.002 mm/s to reach the peak stress in 15 to 30 min. The deformation and the force were registered, including the post-peak softening regime.
Four specimens were tested by applying a *cyclic loading* (Figure 6). This loading scheme gives additional information regarding the loading-unloading behaviour. Five cycles of three runs were applied at approximatively 0.07, 0.1, 0.25, 0.5 and 0.75 of the expected maximum strength. The load was applied with a rate of 0.0075 mm/s to reach the peak stress in approximatively 30 min. The deformation and the force were registered.

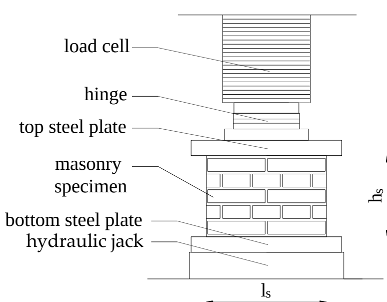

(a)

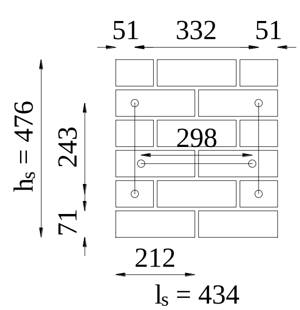

(b)

Figure 5 – Compression test on masonry: (a) test set-up; (b) position of the LVDTs.

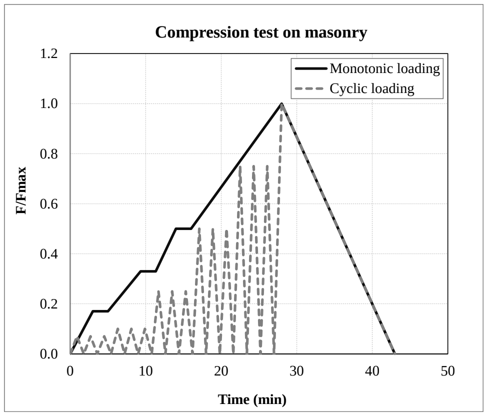

Figure 6 – Monotonic and cyclic loading scheme for compression test on masonry specimen.

6.2 Experimental results

Assuming that the stress is constant over the cross-section of the specimen, the compressive strength of masonry, f'_m, can be determined as follows:

$$f_m^{'} = \frac{F_{\max}}{t_s l_s} \tag{5}$$

where F_{max} is the maximum load, l_s and t_s are the dimensions of the masonry specimen as built (Figure 5).

During the test the displacements and the force were measured continuously allowing the determination of the stress-strain relationship along the loading direction, which was defined as normal direction. Form this relation was possible to determine the elastic modulus of masonry. Three estimates of the elastic modulus were adopted (Figure 7a):

- E_1 is the secant elastic modulus evaluated at 1/3 of the maximum stress;
- E_2 is the secant elastic modulus evaluated at 1/10 of the maximum stress;
- E_3 is the chord elastic modulus evaluated between 1/10 and 1/3 of the maximum stress.

The first estimate was consistent with the prescription of EN 1052-1:1998. The third estimate aimed to exclude the initial start-up of the stress-strain diagram, which would unrealistically affects the other two secant estimates with the initial lower slope.

In the case of cyclic compression tests, aside from the elastic modulus, the stiffness was evaluated for the cycles that were performed in the elastic phase (i.e. 0.07, 0.1, and 0.25 of the expected maximum strength). The cyclic stiffness for each cycle was evaluated as follows: (a) identifying the maximum and minimum stress and strain for each run; (b) taking an average for the specified maximum and minimum points of the three runs; (c) calculating the slope of the line passing through those average points (Figure 7b).

Three estimations of the cyclic stiffness are defined as follows:

- E_{c1} is the cyclic stiffness evaluated in the cycle corresponding to a stress level equal to 0.07 of the expected maximum strength.
- E_{c2} is the cyclic stiffness evaluated in the cycle corresponding to a stress level equal to 0.1 of the expected maximum strength.
- E_{c3} is the cyclic stiffness evaluated in the cycle corresponding to a stress level equal to 0.25 of the expected maximum strength.

The Poisson ratio ν is determined in the elastic phase as the ratio between the lateral strains, which are evaluated in the direction perpendicular to the loading one, and the normal strains (Figure 7c).

The displacement control procedure of the test allowed determining the post-peak behaviour of the material. The fracture energy in compression $G_{f\text{-}c}$ was determined as the area underneath the normal stress versus normal strain diagram, taking the height of the specimen into account. This concept was introduced by van Mier [11] for concrete material and subsequently applied to masonry by Lourenco [12]. In the case of cyclic loading, the envelope curve was considered for the calculation of the fracture energy.

Due to the instinct stiffness of the testing machine, there is a difference between the LVDTs' reading and jack's measurement. Therefore, the LVDTs' readings were used as a basis for evaluating the elastic modulus and the Poisson ratio. Because of extensive cracking in the post-peak phase, LVDTs might be detached from the specimen and there is no measuring data at this phase (Figure 8a). In the previous testing campaign, the fracture energy was calculated considering the jack's measurement.

The fracture energy is evaluated as the area underneath the complete stress-strain relationship along the loading direction. The LVDTs' readings provide the most accurate measurement of the stain; however due to the extensive cracking they may be detached from the specimen during the post-peak phase. Consequently, the jack's measurement should be used to obtain a complete stress-strain relationship. During the measurements, a linear relationship between the LVDTs' reading and jack's readings has been observed in the post-peak phase (Figure 7d). For this reason the complete stress-strain relationship is defined by using both the LVDTs' and jack's readings. Consequently, the complete stress strain relationship is defined as: in the pre-peak phase the LVDTs' readings are adopted, in the post-peak phase the jack's readings are used and modified by imposing that the peak strain defined by the jack's measurement is the same of the one determined by the LVDTs' measurements. The peak strain is defined as the strain corresponding to the maximum stress (Figure 7e).

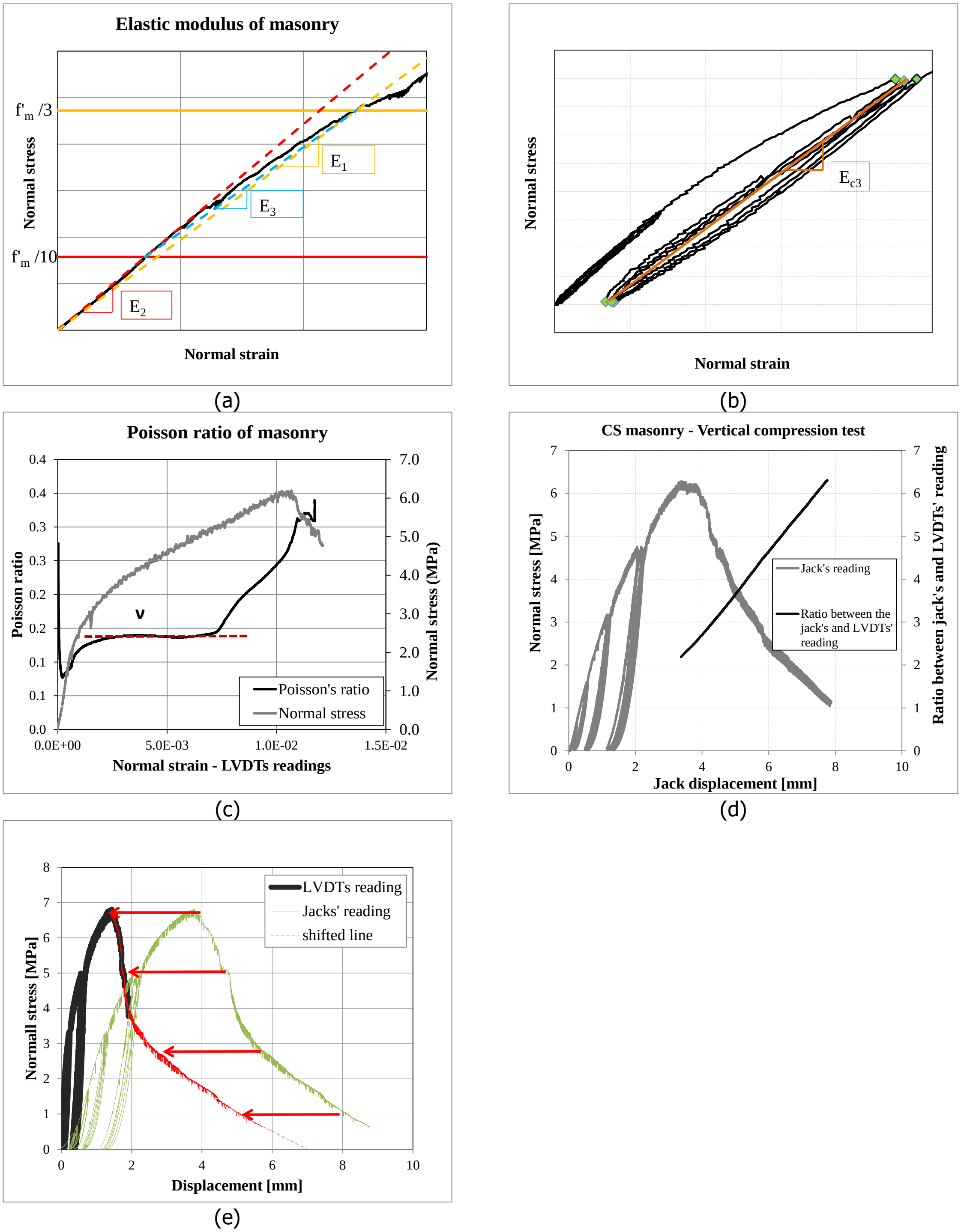

Figure 7 – Compression test on masonry: (a) three estimates of the elastic modulus; (b) estimate of the cyclic stiffness; (c) evaluation of Poisson ratio; (d) comparison between jack's reading and LVDTs' reading in the post-peak phase; (e) adopted method to evaluate the fracture energy.

Figure 8a show the stress-strain diagram for the calcium silicate masonry under vertical compression tests. The graphs refer to the normal direction that is defined as the one parallel to the loading direction.

The pre-peak stage was characterised by linear-elastic followed by a hardening behaviour until the peak. In this stage, the nonlinearity occurred at a stress level approximatively of 1/10 of the maximum stress. After the maximum stress was reached, a softening behaviour was observed. The softening branch was approximatively linear. In the case of cyclic loading, the masonry showed an elastic unloading.

Figure 9 analyses the development of cracks in one specimen tested under vertical compression test. The cracks started at the mortar-brick interface for the joints orthogonal to the loading direction (Figure 9a). When the maximum stress was reached, vertical cracks develop in the bricks. The cracks mainly occurred in the central part of the specimens (Figure 9b). In the post-peak phase, the vertical cracks mainly occurred in the bricks and develops uniformly through the length of the specimen, by splitting it in two parts (Figure 9c, Figure 9d). The cracking was observed to occur in a distributed manner over the height of the specimen; no localisation of the cracking at the boundary was observed.

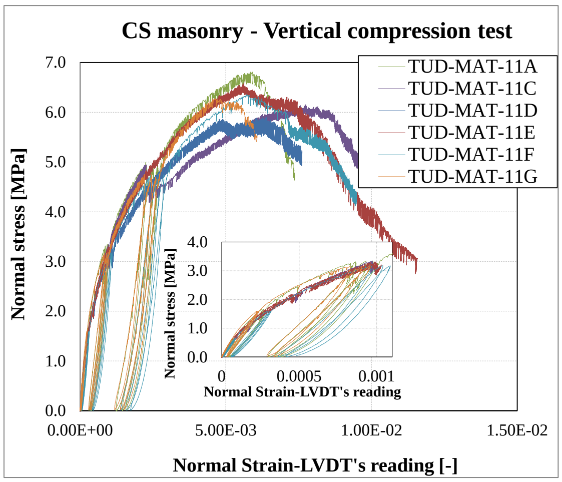

(a)

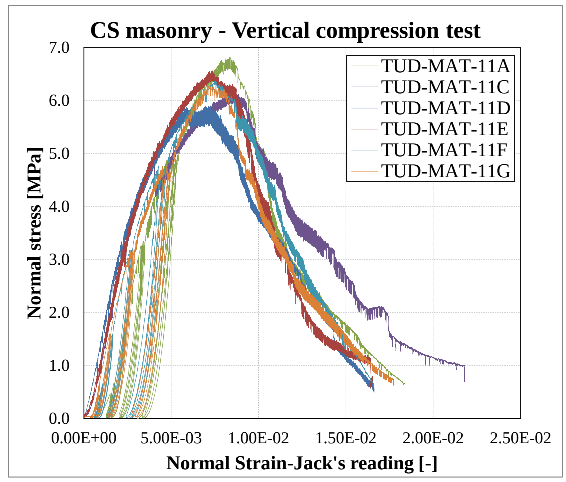

(b)

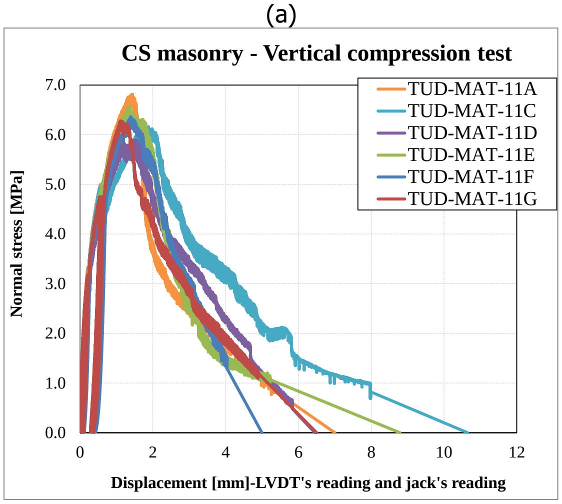

(c)

Figure 8 – Vertical compression tests on calcium silicate masonry specimens: (a) normal strain obtained by LVDTs reading; (b) normal strain obtained by jack's reading; (c) stress- strain curve where the displacement obtained from the LVDTs' reading in the pre-peak phase and jack's reading in the post-peak phase to evaluate the fracture energy.

σ_n= 6.1 MPa, ε_n= 5.5 ‰ (a)　σ_n= 6.4 MPa, ε_n= 5.7 ‰ (b)　σ_n= 1.6 MPa (c)　σ_n= 0.8 MPa (d)

Figure 9 – Crack pattern of specimen TUD_MAT-11F tested under cyclic vertical compression test: (a) first crack; (b) maximum stress; (c)-(d) post-peak phase.

Table 7 lists the main experimental results for the calcium silicate masonry specimens. Figure 10 shows the results with the histogram representation.
The secant elastic modulus E_1 evaluated at 1/3 of the maximum stress and the chord modulus E_3 provided a similar estimation, while the elastic modulus E_2 at 1/10 of the maximum stress provided higher values. This confirms the start of the non-linearity for lower values of normal stress.
The stiffness evaluated at the first, E_{c1}, and the second, E_{c2}, cycle provided a similar estimation, while the stiffness evaluated at the third cycle E_{c3} resulted lower value.
The average Poisson ratio ν was estimated equal to 0.16.

Table 7 – Vertical compression test results on calcium silicate masonry specimens (Aug. 2016).

Specimen name*	**Test type**	***f'_m***	***E_1***	***E_2***	***E_3***	***G_f-c****	***E_c1***	***E_c2***	***E_c3***	***v***
		MPa	MPa	MPa	MPa	N/mm	MPa	MPa	MPa	0.17
TUD_MAT-11A	cyclic	6.81	5274	8391	4550	18.1	9072	8566	6952	0.17
TUD_MAT-11C	monotonic	6.16	4652	6833	4092	26.8	-	-	-	0.11
TUD_MAT-11D	monotonic	5.90	5111	7548	4490	19.4	-	-	-	0.17
TUD_MAT-11E	monotonic	6.58	4485	8778	3708	19.9	-	-	-	-
TUD_MAT-11F	cyclic	6.36	4415	7953	3708	18.0	8522	8313	6159	0.17
TUD_MAT-11G	cyclic	6.27	5895	9736	5043	18.0	10250	9684	7609	-
Average	All	**6.35**	**4972**	**8206**	**4265**	**20.0**	**9281**	**8854**	**6907**	**0.16**
Standard deviation		**0.32**	**568**	**1008**	**527**	**3.43**	**883**	**730**	**726**	**0.03**
Coefficient of variation		**0.05**	**0.11**	**0.12**	**0.12**	**0.17**	**0.10**	**0.08**	**0.11**	**0.19**

* TUD_MAT-11B was subjected to the cyclic load. The results were excluded from the average, since the sample was not straight.

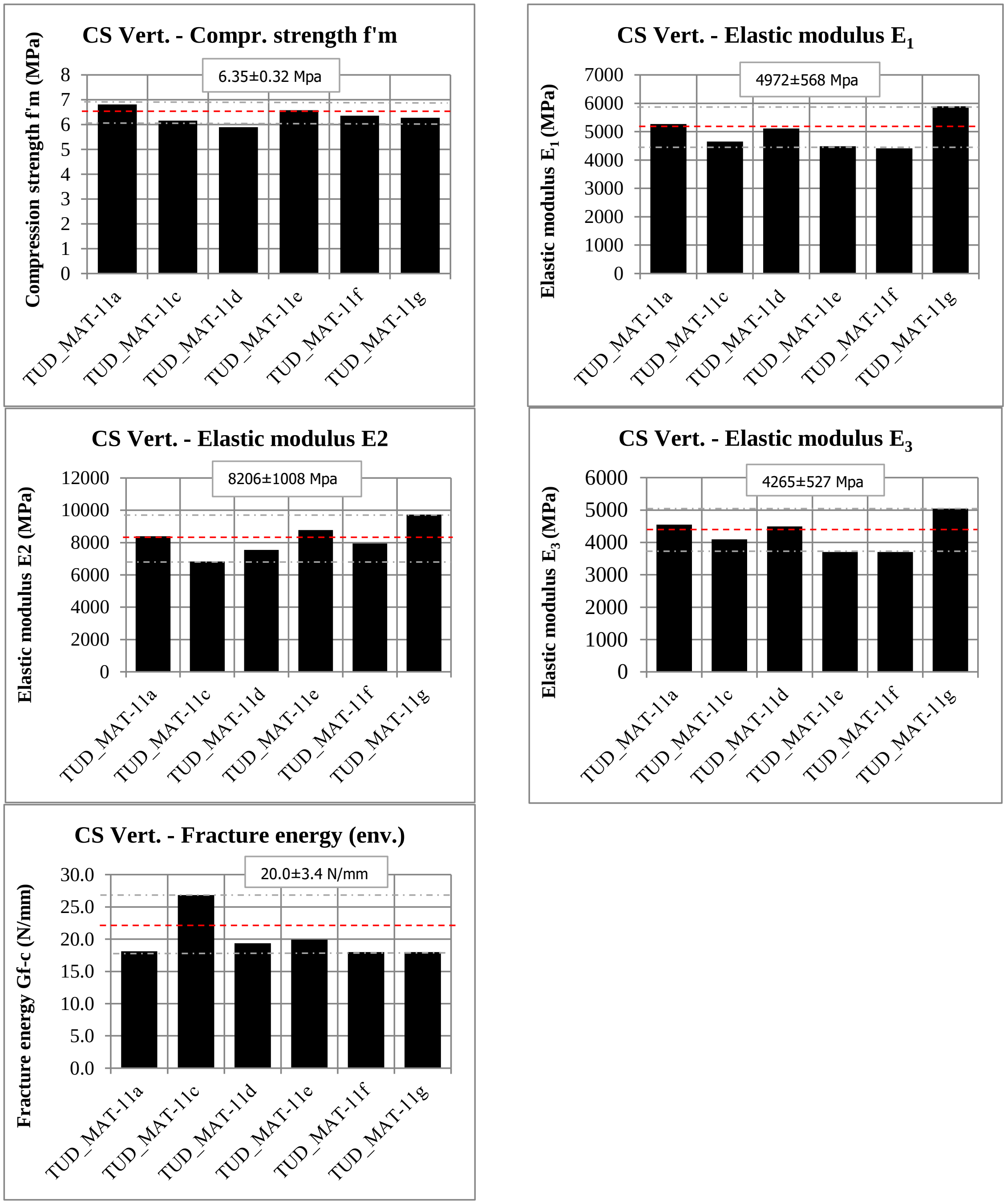

Figure 10 – Vertical compression tests on calcium silicate masonry specimens (third period): histogram

Table 8 shows a comparison between the results of tests on the calcium silicate brick masonry wallets build during the three construction phases. The results of tests on the third phase of construction show slightly higher values for the compressive strength f'_m, while the secant elastic moduli E_1 , E_2 and the elastic modulus E_3 show higher values.

Table 8 – Calcium silicate masonry subject to vertical compression test: comparison between different construction phases.

Series	Statistical parameter	f'_m	E_1	E_2	E_3	v
		MPa	MPa	MPa	MPa	
First period (Apr/May 2015)	Average	**5.93**	**3174**	**5091**	**2746**	**0.14**
	Standard deviation	0.52	467	1774	282	0.01
	Coefficient of variation	0.09	0.15	0.35	0.10	0.07
Second period (Sept. 2015)	Average	**5.76**	**3340**	**4537**	**3005**	**0.18**
	Standard deviation	0.59	800	1888	568	0.07
	Coefficient of variation	0.10	0.24	0.42	0.19	0.41
Third period (Aug. 2016)	Average	**6.35**	**4972**	**8206**	**4265**	**0.16**
	Standard deviation	0.32	568	1008	527	0.03
	Coefficient of variation	0.05	0.11	0.12	0.12	0.19
$(P_{Third}-P_{first}) / P_{Third}$		**0.07**	**0.36**	**0.38**	**0.36**	**0.11**
$(P_{Third}-P_{second}) / P_{Third}$		**0.09**	**0.33**	**0.45**	**0.30**	**-0.15**

Figure 11 shows the envelope curve from the LVDTs' reading for the results of the vertical compression tests on the masonry wallets constructed at three different phases.

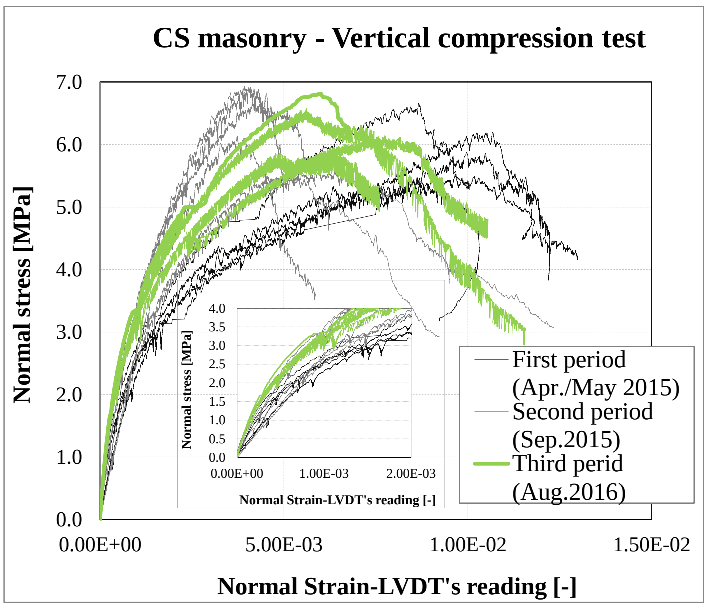

Figure 11 – Vertical compression tests on the calcium silicate masonry specimens constructed at three construction periods.

7 Bond strength of masonry

The bond strength between masonry unit and mortar was determined in agreement with the bond wrench test proposed by EN 1052-5:2002 [13].

7.1 Testing procedure

The test set-up used in the previous experimental campaign in 2015 is shown in Figure 12a. In this set-up a lever was used to apply a bending moment to the brick-mortar interface. The applied moment was registered on an analogue scale. The apparatus was officially calibrated in the range 20–215 Nm, with a tolerance of 4%.
Due to the difficulties of dealing with the retaining frame, the bond wrench set-up used in the previous campaigns was improved. The improved set-up used in the current campaign is shown in Figure 12b. The specimen is rigidly held by a support frame that holds the specimen in accordance with EN 1052-5:2005 [13]. A clamp, with a lever attached, was applied to the masonry unit above the tested. The lever was used to apply a bending moment to the brick-mortar interface. The load was applied by a jack operated manually and a load cell attached to the jack measures the applied force. Therefore, the improved set-up provides the possibility for registering the load as well as applying higher range of load, in particular for the samples with the higher value of bond strength (e.g. calcium silicate element).
A couplet specimen was adopted for the bond wrench tests (Figure 12c).

(a) (b) (c)

Figure 12 – Bond wrench tests: (a) bond wrench set-up used in the previous campaigns; (b) improved bond wrench set-up used in this campaign; (c) couplet specimen.

7.2 Experimental results

The bond wrench strength f_w is calculated on the assumption that the stress distribution is linear over the width of the top masonry unit [13]:

$$f_w = \frac{F_1 e_1 + F_2 e_2 - \frac{2}{3} t_u \left(F_1 + F_2 + \frac{F_3}{4} \right)}{l_j w_j^2 / 6} \tag{6}$$

where F_1 is the failure load, measured and applied by the jack. F_2 is the normal force as a result of the weight of the bond wrench apparatus (F_2 = 50.9 N). F_3 is the weight of the masonry unit pulled off the specimen, including the weight of adherent mortar. Furthermore, e_1 is the distance from the applied load to the tension face of the specimen, e_2 is the distance from the centre of gravity of the clamp to the tension face of the specimen, l_j is the mean length of the bed joint, and w_j is the mean width of the bed joint. Figure 13 show the set-up and the definition of the various quantities.

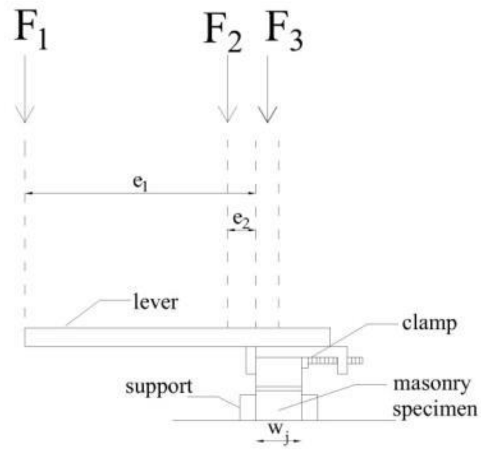

Figure 13 – Test set-up for the bond wrench test.

Figure 14 reports the classification of the type of failures [13], while Figure 15 shows the observed failure mechanisms.

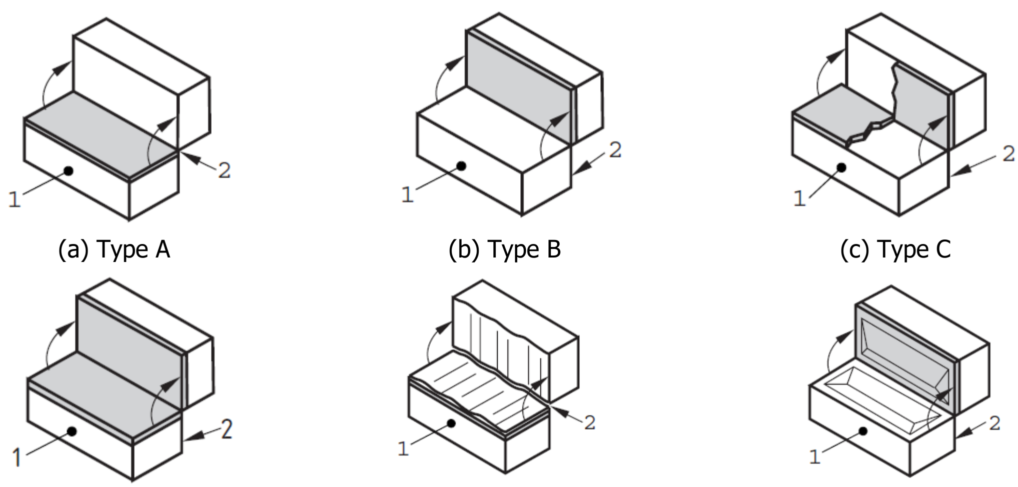

(a) Type A (b) Type B (c) Type C

(d) Type D (e) Type E (f) Type F

Figure 14 – Classification of failure modes in agreement with EN-1052-5:2005 (1 tension face, 2 compression face).

(a) (b)

Figure 15 – Observed failure mechanisms: (a) type A; (b) type B.

Figure 16 shows the applied load (F_1) versus time. From the graph the brittle behaviour of the samples are clear.

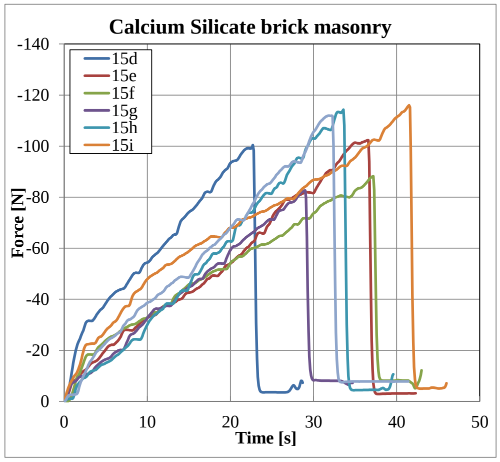

Figure 16 – Time versus force (F1) applied by manually controlled jack.

Table 9 lists the results of the calcium silicate masonry. Three samples 15a-15b-15c showed detachment of the two brick during the installation of the specimen in the set-up; consequently they are not considered in the statistical analysis.

Table 9 – Bond strength of calcium silicate masonry samples (Aug.2016).

Specimen Name*	**Maturation**	**l_j**	**w_j**	**F_3**	**F_1**	**f_w**	**Failure mode**
	days	mm	mm	N	N	MPa	
15d	81	210	101	21.2	100.51	0.12	A
15e	81	209	101	22.4	102.41	0.12	A
15f	81	210	100	36.2	88.24	0.11	B
15g	81	210	101	37.0	82.61	0.10	B
15h	81	210	101	38.7	114.43	0.13	B
15i	81	209	102	38.9	116.13	0.13	B
15j	81	209	102	21.7	104.80	0.12	A
				average		**0.12**	
				st. dev.		**0.01**	
				c.o.v.		**0.12**	

* Complete specimen name starting with TUD_MAT-.

Table 10 lists an overview of the bond wrench test results for the calcium silicate masonry samples tested at different phases of construction. It can be observed that the results correlated to the third construction phase show a significant lower coefficient of variation. This improvement can be addressed to the change in set-up from manual to automatic control.
Figure 17 shows the results in terms of probability distribution function.

Table 10 – Comparison between the bond wrench test results obtained in the three construction phases.

Period	No. Specimens	f_w		
		Average (MPa)	**St. dev.**	**C.o.V.**
First phase (Apr/May 2015)	35	**0.27**	0.12	0.43
Second phase (Sept. 2015)	36	**0.28**	0.08	0.29
Third phase (Aug. 2016)	7	**0.12**	0.01	0.12

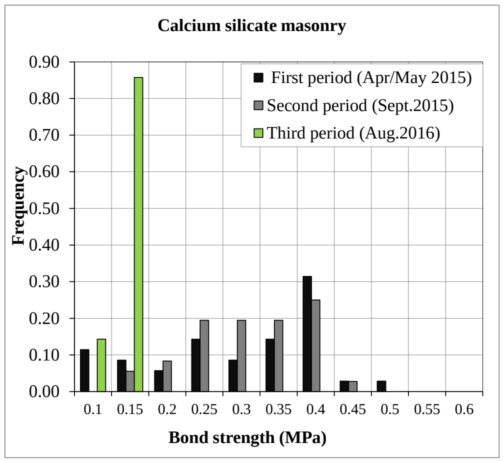

Figure 17 – Probability distribution functions of bond strength for calcium silicate masonry sample for three phases of construction.

8 Shear strength of masonry

The initial shear properties of masonry were determined in agreement with EN 1052-3:2002 [14]. However, a displacement control procedure was used, instead of the prescribed force control procedure, to evaluate the residual strength properties and the mode-II fracture energy.

8.1 Testing procedure

Two types of specimens, standard triplet and modified triplet, were adopted. Fourteen specimens for each type of triplet were prepared. The standard triplet is a three stacked bonded brick specimen (Figure 19a), while the modified triplet is formed by bricks bonded in different patterns (Figure 19b). Prior to testing, a layer of gypsum was applied to the external faces of the specimens.

Figure 18 shows the used test set-up. During the test, the specimen was rotated of 90 degrees with respect to the casting position. The specimen was kept under constant lateral pre-compression, while a shear load was applied at the mid masonry unit. Three different levels of pre-compression were investigated. Being the compressive strength of the masonry unit greater than 10 N/mm^2 [14], the pre-compression stresses applied were 0.2, 0.6 and 1.0 N/mm^2. For each pre-compression level, three specimens were tested.

Two independently operated jacks were required to apply the shear and pre-compressive load. The shear load acts in a vertical direction using a displacement controlled apparatus. The apparatus has a 100 kN jack and a spherical joint. The displacement increased with a rate of 0.005 mm/s. During unloading, the displacement was decreased with a rate of 0.05 mm/s. The pre-compressive load was applied perpendicular to the bed joint plane by a manually operated hydraulic jack. The horizontal hydraulic jack was load controlled and applied different levels of transverse compressive load to the specimen. The jack was kept in position by means of four steel rods positioned on opposite sides of the specimen, which were in turn kept in position by steel plates (Figure 18). In order to keep the transverse compressive load constant (±2%), a spring system is used between the hydraulic jack and the load cell. The stiffness of the springs is defined on the basis of the required pre-compression level. Two types of the spring having the stiffness of 123 N/mm and 3300 N/mm were used. A load cell is placed between the spring and the steel plate to measure the applied load.

Both on the front and the back side of the specimens, LVDTs are attached. Vertical LVDTs measure the relative vertical displacement of the middle brick with respect to the later ones. Horizontal LVDTs measures the horizontal displacement between the two external bricks. Their measuring range is 10 mm with an accuracy of 0.5% (Figure 19).

In order to follow the same testing procedure for the shove test, the pre-compression load was increased and kept constant at different levels in the residual phases.

In order to get more insight into the initial shear strength, one sample for each type of triplets was tested at a very low pre-compressive stress of 0.05 MPa.

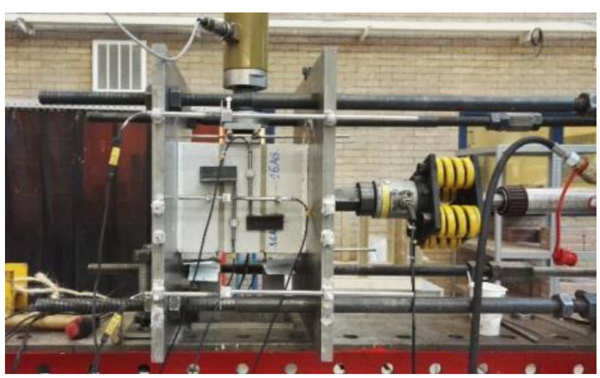

Figure 18 – Test set-up for the shear-compression test on masonry specimen.

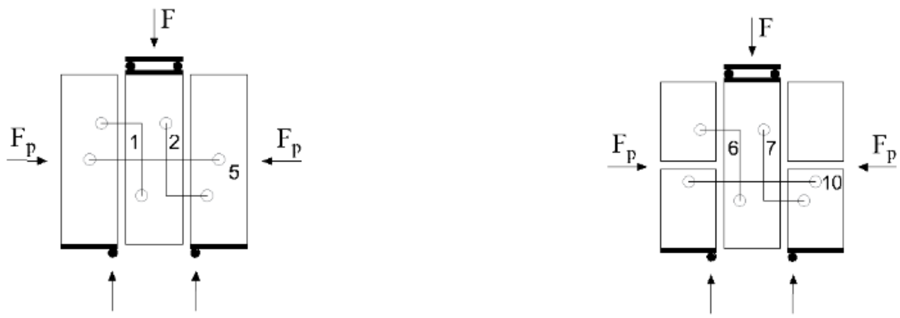

Figure 19 – Specimens adopted for shear-compression test: (a) standard triplets; (b) modified triplets.

8.2 Experimental results

The shear strength f_v was calculated for each specimen as follows [14]:

$$f_v = \frac{F_{\max}}{2A_s} \tag{7}$$

where F_{max} is the maximum load, A_s is the cross sectional area of the specimen parallel to the bed joints.
The pre-compression stress f_p can be calculated for each specimen as follows [14]:

$$f_p = \frac{F_p}{A_s} \tag{8}$$

where F_p is the pre-compression force.

The test was carried out in displacement control allowing for the determination of the post-peak behaviour. As a consequence, the residual shear strength $f_{v,res}$ was also determined. The residual strength occurred at an almost constant load where a plateau of large sliding displacement was observed. The resistance in the post-peak phase can be associated to friction only, since large relative displacement occurs.

The results of all the tests were plotted in a pre-compressive stress versus shear strength diagram. Considering a linear regression of the date, the initial shear strength f_{v0} and the coefficient of friction μ can be found such as the intercept with the vertical axis and the gradient of the line, respectively. The angle of internal friction α was determined as the angle between the regression line and the horizontal axis.
Similar consideration can be applied to determine the residual shear strength $f_{v0,res}$ and the residual coefficient of friction μ_{res}. In the Coulomb friction formulation, the result is:

$$f_v = f_{v0} + \mu f_p \tag{9}$$

$$f_{v,res} = f_{v0,res} + \mu_{res} f_p \tag{10}$$

Table 11 and Figure 20 show the results for *standard triplets.* The calcium silicate masonry showed an initial shear strength equal to 0.11 MPa and a coefficient of friction equal to 0.52. In the residual phase, the coefficient of friction increased to 0.55. All the specimens presented a shear failure in the unit/mortar bond area. Figure 22 shows a typical crack pattern.

Table 12 and Figure 21 show the results for *modified triplets*. The calcium silicate masonry showed an initial shear strength equal to 0.18 MPa and a coefficient of friction equal to 0.46. In the residual phase, the coefficient of friction increased to 0.47. All the specimens presented a shear failure in the unit/mortar bond area. Figure 23 shows a typical crack pattern.

Table 11 - Maximum and residual shear strength and mode-II fracture energy of standard triplets.

f_p = 0.2 MPa				f_p = 0.6 MPa				f_p = 1.2 MPa			
Specimen name(*)	f_v	$f_{v,res}$	$G_{f\text{-}II}$	**Specimen name(*)**	f_v	$f_{v,res}$	$G_{f\text{-}II}$	**Specimen name(*)**	f_v	$f_{v,res}$	$G_{f\text{-}II}$
	MPa	MPa	N/mm		MPa	MPa	N/mm		MPa	MPa	N/mm
16AF	0.21	0.11	0.022	16AD	0.47	0.35	0.085	16AB	0.69	0.67	0.014
16AI	0.18	0.13	0.012	16AG	0.44	0.33	0.054	16AE	0.74	0.67	0.111
16AO	0.19	0.11	0.024	16AM	0.45	0.33	0.067	16AL	0.70	0.62	0.341
Average	**0.19**	**0.12**	**0.02**	Average	**0.45**	**0.34**	**0.07**	Average	**0.71**	**0.65**	**0.16**
St. dev.	**0.02**	**0.01**	**0.01**	St. dev.	**0.02**	**0.01**	**0.02**	St. dev.	**0.03**	**0.03**	**0.17**
C.o.V.	**0.08**	**0.11**	**0.33**	C.o.V.	**0.03**	**0.03**	**0.23**	C.o.V.	**0.04**	**0.04**	**1.08**

(*) Complete specimen name starting with TUD_MAT-.

Table 12 - Maximum and residual shear strength and mode-II fracture energy of modified triplets.

f_p = 0.2 MPa				f_p = 0.6 MPa				f_p = 1.2 MPa			
Specimen name(*)	f_v	$f_{v,res}$	$G_{f\text{-}II}$	**Specimen name(*)**	f_v	$f_{v,res}$	$G_{f\text{-}II}$	**Specimen name(*)**	f_v	$f_{v,res}$	$G_{f\text{-}II}$
	MPa	MPa	N/mm		MPa	MPa	N/mm		MPa	MPa	N/mm
16BF	0.22	0.12	0.034	16BD	0.47	0.34	0.094	16BC	0.69	0.52	1.036
16BH	0.25	0.12	0.046	16BE	0.48	0.33	0.096	16BG	0.73	0.60	0.368
16BI	0.33	0.11	0.076	16BN	0.42	0.32	0.221	16BA	0.72	0.62	0.011
Average	**0.27**	**0.12**	**0.05**	Average	**0.46**	**0.33**	**0.14**	Average	**0.71**	**0.58**	**0.47**
St. dev.	**0.06**	**0.01**	**0.02**	St. dev.	**0.03**	**0.01**	**0.07**	St. dev.	**0.02**	**0.05**	**0.52**
C.o.V.	**0.22**	**0.05**	**0.42**	C.o.V.	**0.08**	**0.03**	**0.53**	C.o.V.	**0.03**	**0.09**	**-**

(*) Complete specimen name starting with TUD_MAT-.

Table 13 lists the shear properties for both the standard and modified triplet tests. It should be mentioned that instead of applying 1.0 MPa pre-compression stress (suggested by the standards), the pre-compression stress of 1.2 MPa was applied for both tests on the standard and modified triplets. In the case of testing on the modified triplet specimens, one sample was tested at pre-compressive stress of 1.0 MPa; the results are in line with the test performed for pre-compression level of 1.2 MPa.
The initial shear strength obtained from the tests on the standard triplets shows lower values than the initial shear strength obtained from the tests on the modified triplets. The coefficient of friction for the standard triplets shows higher value than those of modified triplets. Although, there is a deference between the obtained results from tests on the two types of the adopted samples, the results of modified triplets are almost in line with those of standard triplets.

Table 13 - Shear properties of standard triplets and modified triplets.

Property	**Symbol**	**Unit**	**Standard triplets**	**Modified triplets**
Initial shear strength	f_{v0}	MPa	0.11	0.18
Coefficient of friction	μ		0.52	0.46
Angle of internal friction	α		27.5°	24.7°
Residual shear strength	$f_{res,v}$	MPa	0.01	0.03
Residual coefficient of friction	μ_{res}		0.55	0.48
Residual angle of internal friction	α_{res}		28.8°	25.6°

.

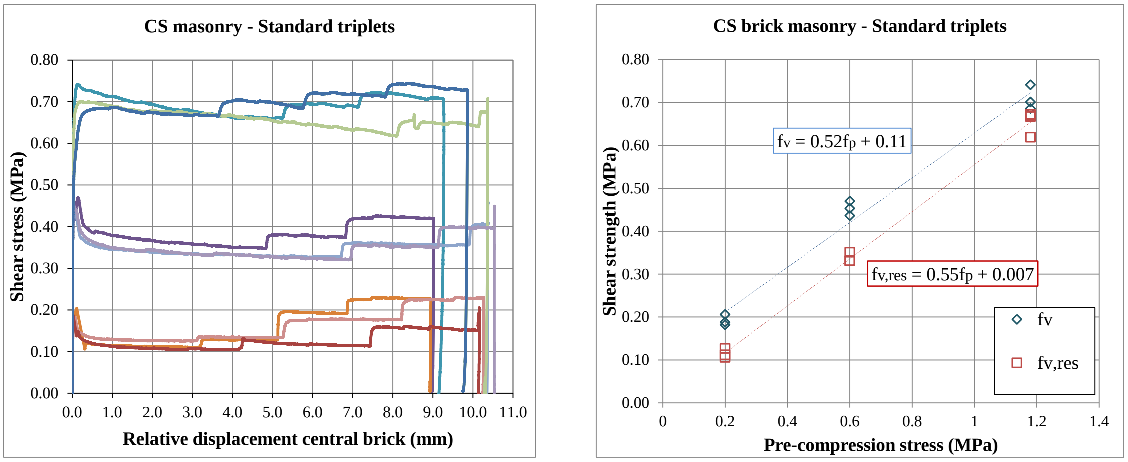

(a) (b)

Figure 20 – Shear test results for standard triplets: (a) shear stress versus relative displacement of the central brick (LVDTs readings); (b) shear strength versus pre-compression stress.

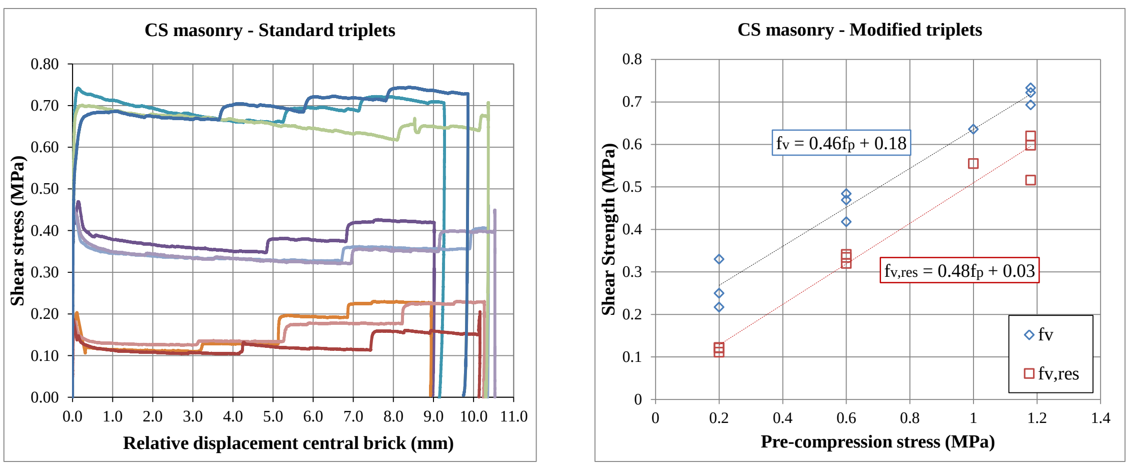

(a) (b)

Figure 21 – Shear test results for modified triplets: (a) shear stress versus relative displacement of the central brick (LVDTs readings); (b) shear strength versus pre-compression stress.

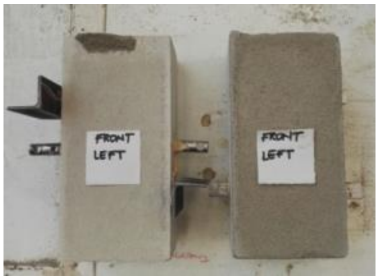

(a)

(b)

(c)

Figure 22 – Crack pattern of standard triplets under shear test: (a) front-left joint; (b) front-right joint; (c) front view.

(a)

(b)

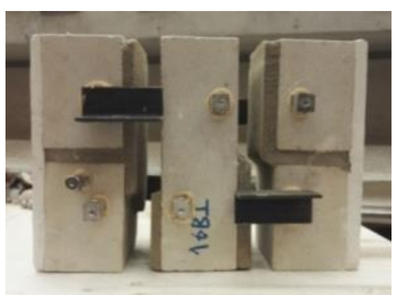

(c)

Figure 23 – Crack pattern of modified triplets under shear test: (a) front-left joint; (b) front-right joint; (c) front view.

The tests on triplets were aimed to have a sufficiently reliable measure of the bed joint shear strengths under controlled normal stress. These results will be used as a benchmark for the interpretation of the shove tests. In order to get better insight into the initial shear strength, one sample for each type of triplet was tested at a very low pre-compressive stress of 0.05 MPa. The measured data are shown in Figure 24 with dark blue dots. To get more precise envelope at residual state, the pre-compression load was increased and kept constant at different levels in the residual phases. The measured data are shown in Figure 24 with red filled dots.

Figure 24 shows the shear properties for the standard and modified triplet tests, compiling the data measured according to the testing protocols and all the data including the additional ones measured for the correlation purposes.

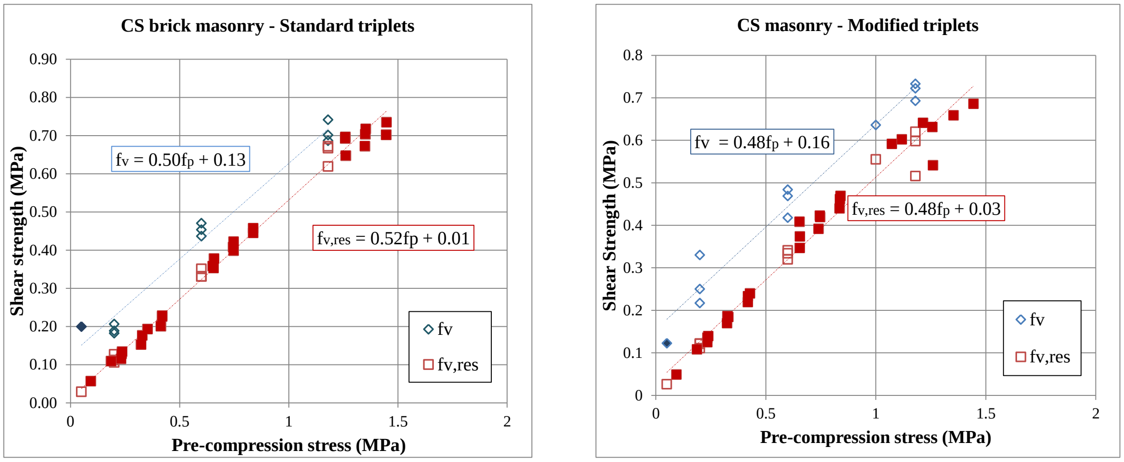

(a) (b)

Figure 24 – Shear strength versus pre-compression stress for all the measured data: (a) standard triplet; (b) modified triplet.

Table 14 shows the comparison between the shear properties of the standard triplet specimens build in the first construction phase and the standard triplet build in the third construction phase. The shear properties for the third construction phase are reported considering all the measured data, as shown in Figure 24. Similar initial shear strength is obtained in the two periods, while an increase of the coefficient of friction is observed for the specimens build in the third construction phase. Additionally, for the specimens build in the third construction phase the coefficient of friction is constant both for the initial and residual stresses, while for the specimens build in the first construction phase a friction-hardening behaviour was observed.

Table 14 - Comparison between the results of tests on standard triplets at two phases of construction.

Property	**Symbol**	**Unit**	**First phase (Apr/May2015)**	**Third phase (Aug. 2016)**
Initial shear strength	f^{*}_{v0}	MPa	0.14	0.13
Coefficient of friction	μ^{*}		0.43	0.50
Angle of internal friction	α^{*}		23°	26.6°
Residual initial shear strength	$f^{*}_{res,v0}$	MPa	0.03	0.01
Residual coefficient of friction	μ^{*}_{res}		0.54	0.52
Residual angle of internal friction	α^{*}_{res}		28°	27.5°

9 Summary and properties overview

The main goal of the WP1a is to qualify the firms with respect to the in-situ activities, while the sub-goal is to study the correlation between destructive tests (DT) and non/slightly destructive tests (NDT/SDT). As a result, NDT/SDT were performed in a controlled laboratory environment on the replicated calcium silicate brick masonry walls. In addition, DT were performed on the companion samples by TUDelft. This document reports the material properties of CS brick masonry by performing DTs on the replicated specimens. These material properties reported in this document can be used to further study the correlation between NDT and SDT, as well as to be used as a benchmark to interpret the obtained results of SDT (e.g. shove test).

Characterising the material properties of CS brick masonry have been planned in the large-scale testing campaign of 2015, at TU Delft. The material characterisation of masonry was performed by investigating its behaviour under compressive, bending and shear loading. For every type of test, both the maximum capacity of the masonry and the stress-strain relationship were investigated. To characterise the orthotropic behaviour of masonry, both compressive and out-of-plane bending tests were performed along two loading directions: one generating cracking parallel to the bed joints and one generating cracking perpendicular to the bed joints. The tests were performed in two periods: in the first construction period (March-April 2015) specimens for the material (MAT) and component tests (COMP) were built, while in the second period (September 2015) the construction of the assemblage took place, and a limited number of material tests was repeated. The results of the second testing period are in line with the one obtained in the first period, as shown in Table 15. As a result, the complete overview of the behaviour of CS brick masonry has been established in the large-scale testing campaign of 2015.

In the pre-qualification project, the companion samples were constructed, aside from the large-scale walls adopted for the NDT/SDT testing activities by firms. The companion samples were adopted with the aim to be subjected to DT. The results of the last testing period are listed in Table 15. The compressive strength of mortar, the compressive strength of masonry and the shear properties obtained in the last construction period are in line with those obtained in the first and second periods. On the contrary, the obtained values of the Young's modulus are higher than those measured in the previous periods. This difference can be inputted to the different environmental conditions, the mixing technique adopted for the mortar and the aging of the pre-mix mortar. The average of the obtained results at different construction periods are reported in Table 15 and can be used as a benchmark to reflect on the behaviour of the CS brick masonry studied in the WP1a.

Table 15 – Overview of mechanical properties for calcium silicate masonry.

Property		Symbol	Unit	Calcium silicate masonry											
				First period (Mar/Apr 2015)			Second period (Sept 2015)			Third period (Aug 2016)			All results		
				Average	St. dev.	C.o.V.	Average	St. dev.	C.o.V.	Average	St. dev.	C.o.V.	Average	St. dev.	C.o.V.
Compressive strength of mortar		f_m	MPa	**6.59**	0.66	0.10	**7.24**	0.60	0.08	**7.57**	0.46	0.06	**7.27**	1.02	0.14
Flexural strength of mortar		f_{mt}	MPa	**2.79**	0.22	0.08	**3.56**	0.18	0.05	**3.21**	0.18	0.05	**3.11**	0.36	0.12
Normalised compressive strength of masonry unit		f_b	MPa	-	-	-	-	-	-	**13.26**	1.71	0.13	**13.26**	1.71	0.13
Compressive strength of masonry in the direction perpendicular to bed joints		f'_m	MPa	**5.93**	0.52	0.09	**5.76**	0.59	0.10	**6.35**	0.32	0.05	**6.01**	0.53	0.09
Elastic modulus of masonry in the direction perpendicular to bed joints		E_1	MPa	**3174**	467	0.15	**3340**	800	0.24	**4972**	568	0.11	**3828**	1033	0.27
		E_2	MPa	**5091**	1774	0.35	**4536**	1888	0.42	**8206**	1008	0.12	**5945**	2260	0.38
		E_3	MPa	**2746**	282	0.10	**3005**	568	0.19	**4265**	527	0.12	**3339**	824	0.25
Cyclic modulus of masonry in the direction perpendicular to bed joints		E_{c1}	MPa	-	-	-	-	-	-	**9281**	883	0.10	**9281**	883	0.10
		E_{c2}	MPa	-	-	-	-	-	-	**8854**	730	0.08	**8854**	730	0.08
		E_{c3}	MPa	-	-	-	-	-	-	**6907**	726	0.11	**6907**	726	0.11
Poisson ratio of masonry in the direction perpendicular to bed joints		ν		**0.14**	0.01	0.07	**0.18**	0.07	0.41	**0.16**	0.03	0.19	**0.16**	0.05	0.32
Fracture energy in compression for loading perpendicular to bed joints*		$G_{f\text{-}c}$	N/mm	**31.5**	5.1	0.16	**21.8**	3.6	0.17	**20.0**	3.43	0.17	**20.0**	3.43	0.17
Flexural bond strength		f_w	MPa	**0.27**	0.12	0.43	**0.28**	0.08	0.29	**0.12**	0.01	0.12	**0.26**	0.11	0.40
Masonry (bed joint) initial shear strength	standard triplets	f_{v0}	MPa	**0.14**	-	-	-	-	-	**0.13**	-	-	**0.14**	0.007	0.05
	modified triplets	f^*_{v0}		-	-	-	-	-	-	**0.16**	-	-	**0.16**	-	-
Masonry (bed joint) shear friction coefficient	standard triplets	μ		**0.43**	-	-	-	-	-	**0.50**	-	-	**0.47**	0.05	0.11
	modified triplets	μ^*		-	-	-	-	-	-	**0.48**	-	-	**0.48**	-	-
Residual masonry (bed joint) shear strength	standard triplets	$f_{v0,res}$	MPa	**0.03**	-	-	-	-	-	**0.01**	-	-	**0.02**	0.01	0.71
	modified triplets	$f^*_{v0,res}$		-	-	-	-	-	-	**0.03**	-	-	**0.03**	-	-
Residual masonry (bed joint) shear friction coefficient	standard triplets	μ_{res}		**0.54**	-	-	-	-	-	**0.52**	-	-	**0.53**	0.01	0.03
	modified triplets	μ^*_{res}		-	-	-	-	-	-	**0.48**	-	-	**0.48**	-	-

* Different methods were adopted to evaluate the fracture energy in the last campaigns and current campaign. Therefore, only the results of the current campaign are reported in the average of all results.

References

[1] Esposito R., Messali F., Crielaard R., Rots J.G. "Tests for the characterization of replicated masonry, Delft University of Technology, Dept. Structural Engineering, April 2016.

[2] EN 1996-1-1+A1 (2013). Eurocode 6 – Design of masonry structures – Part 1-1: General rules for reinforced and unreinforced masonry structures. Nederlands Normalisatie-instituit (NEN).

[3] Protocol for the construction of masonry, ver. 18-03-2015.

[4] EN 1015-3 (1999). Method of test for mortar for masonry – Part 3: Determination of consistence of fresh mortar (by flow table). Nederlands Normalisatie-instituit (NEN).

[5] EN 1015-11 (1999). Method of test for mortar for masonry – Part 11: Determination of flexural strength of hardened mortar. Nederlands Normalisatie-instituit (NEN).

[6] EN 772-1 (2000). Methods of test for masonry units - Part 1: Determination of compressive strength. Nederlands Normalisatie-instituit (NEN).

[7] Ad Vermeltfoort. (2005) Brick-mortar interaction in masonry under compression, PhD thesis, Eindhoven University of Technology.

[8] Jafari, S., Panoutsopoulou, L. and Rots, J.G. Tests for the characterisation of original Groningen masonry. Delft University of Technology. Final report 18 December 2015.

[9] EN 1052-1 (1998). Method of test masonry – Part 1: Determination of compressive strength. Nederlands Normalisatie-instituit (NEN).

[10] Procedures of in-situ test. Protocol for the in-situ testing of masonry. 2015; EUCentre Foundation and Risk Centre Pavia.

[11] Van Mier, J.G.M. (1984) Strain Softening of concrete under multiaxial loading conditions, PhD thesis, Eindhoven University of Technology.

[12] Lourenco, P.B., De Borst, R. and Rots, J.G. (1997). A plane stress softening plasticity model for orthotropic materials. International Journal for Numerical Methods in Engineering 40(21), 4033-4057.

[13] EN 1052-5 (2005). Method of test masonry – Part 5: Determination of bond strength by bond wrench method. Nederlands Normalisatie-instituit (NEN).

[14] EN 1052-3 (2002). Method of test masonry – Part 3: Determination of initial shear strength. Nederlands Normalisatie-instituit (NEN).

Appendix A

This appendix reports the declaration of performance for the construction materials used during the experimental campaign.
Table A.1 refers to the calcium silicate bricks.
Table A.2 lists the characteristic of mortars for calcium silicate masonry.

Table A.1 – Declaration of performance of calcium silicate bricks (www.calduran.nl/producten/stenen/).

Wanddikte in mm	Type steen	Afmetingen (BxHxL) mm	Gewicht per stuk in kg	Druksterkte N/mm^2	Aantal per m^2 (incl. voeg)	Kg Metselfix per m^2 excl. morsverlies
55 (klamp)	Waalformaat	102x55x214	2	16	39,9	12,3
72 (klamp)	Amstelformaat	102x72x214	3	16	39,9	16,1
82 (klamp)	Maasformaat	102x82x214	3	16	39,9	18,4
102	Waalformaat	102x55x214	2	16	68,7	33,7
102	Amstelformaat	102x72x214	3	16	54,4	28,3
102	Maasformaat	102x82x214	3	16	48,5	26,1
150	Dubbel amstelformaat	150x72x214	4	16	54,4	42,5
150	Dubbel maasformaat	150x82x214	5	16	48,5	39,2

Table A.2 – Declaration of performance for calcium silicate masonry mortar (www.remix.nl)

1. Unieke identificatie	**Sakrete Brickfix**	**Nr. RV001 – 2013-11-05**
2. Aanduiding	**M5 type G (voor algemene toepassing) conform NEN-EN 998-2: 2010**	
3. Toepassing	**Metselmortel voor binnen- en buitentoepassing**	
4. Naam en contactadres fabrikant	**Remix Droge Mortel BV** **Hoofdstraat 41 NL-9531 AB Borger** **Postbus 3 NL-9530 AA Borger**	
5. Naam en contactadres gemachtigde	geen	
6. Systeem voor de beoordeling en verificatie van de prestatiebestendigheid	systeem 2+	
7. Activiteit van de aangemelde certificatie-instantie zoals vereist in de geharmoniseerde norm	De aangemelde certificatie-instantie Kiwa BMC B.V. (identificatienummer 0620) heeft onder systeem 2+ de initiële inspectie van de productie-installatie en van de productiecontrole in de fabriek uitgevoerd en zal tevens de permanente bewaking, beoordeling en evaluatie van de productiecontrole op zich nemen. Op basis daarvan is het conformiteitscertificaat voor de productiecontrole in de fabriek verstrekt.	
8. Europese Technische beoordeling	niet van toepassing	
9. Aangegeven prestaties		
Essentiële kenmerken (NEN-EN 998-2)	**Prestaties**	**Europees beoordelingsdocument**
5.4.1 druksterkte	M5	NEN-EN 998-2:2010
5.4.2 Hechtsterkte (kruisproef)	≥ 0,3 N/mm² (tabelwaarde)	
5.2.2 chloridegehalte	< 0,1 M.-%	
5.6 brandklasse	A1	
5.3.3 waterabsorptie	≤ 0,40 kg/(m²*min0,5)	
5.4.4 waterdampdoorlaatbaarheid	15/35 (tabelwaarde)	
5.4.6 warmtegeleidbaarheid	≤ 0,82 W/(m*K) P = 50% ≤ 0,89 W/(m*K) P = 90% (tabelwaarden)	
5.4.7 duurzaamheid	NPD	
vrijkomende gevaarlijke bestanddelen	NPD	

10. De prestaties van het in de punten 1 en 2 omschreven product zijn conform de in punt 9 aangegeven prestaties. Deze prestatieverklaring wordt verstrekt onder de exclusieve verantwoordelijkheid van de in punt 4 vermelde fabrikant.

Borger, 5 November 2013

Getekend: AGAR Holding BV

Mr. R.M.P.P. Reef
Algemeen directeur

Remix Droge Mortel BV is een werkmaatschappij van Agar Holding BV.